PROCEEDINGS OF SCIENCE

Observation of a family of all-charm tetraquarks with spin-2 and positive parity at CMS

Xining Wang[a,*]

[a] *Department of Physics, Tsinghua University,*
30 Shuangqing Road, Beijing, China

E-mail: xining.wang@cern.ch

A comprehensive study of all-charm tetraquark candidates is presented in this paper. The search is performed in the $J/\psi J/\psi$ mass spectrum using proton–proton collision data at $\sqrt{s}$ = 13 and 13.6 TeV collected with the CMS detector at the LHC. With about 3.6 times more $J/\psi J/\psi$ pairs compared to the Run 2 dataset alone, the combined Run 2 (2016–2018) and Run 3 (2022–2024) sample provides significantly improved sensitivity to rare structures. In the $J/\psi J/\psi \to \mu^+\mu^-\mu^+\mu^-$ channel, three structures are observed each with a significance well above 5σ, denoted $X(6600)$, $X(6900)$, and $X(7100)$, consistent with the earlier Run 2 observation. In addition, quantum interferences between these states are observed, each with a significance above 5σ, implying they share the same spin–parity quantum numbers. In addition, a search is conducted in the $J/\psi\psi(2S) \to \mu^+\mu^-\mu^+\mu^-$ channel, revealing two structures with masses and widths consistent with $X(6900)$ and $X(7100)$. To further explore the nature of these states, a spin–parity measurement is conducted with the Run 2 $J/\psi J/\psi$ data. Assuming common quantum numbers for the three states, as motivated by the interference pattern, the results favor a $J^{PC} = 2^{++}$ assignment—an unusual quantum number among known hadrons. The combined features of these analyses point to a coherent picture in which the $J/\psi J/\psi$ states observed by CMS constitute a family of all-charm tetraquarks, favoring a diquark-antidiquark structure in which both diquarks are in a spin-1 state and aligned. The findings provide new insights into the internal dynamics of exotic resonances.

The European Physical Society Conference on High Energy Physics (EPS-HEP2025)
7-11 July 2025
Marseille, France

*Speaker

© Copyright owned by the author(s) under the terms of the Creative Commons Attribution-NonCommercial-NoDerivatives 4.0 International License (CC BY-NC-ND 4.0) All rights for text and data mining, AI training, and similar technologies for commercial purposes, are reserved. ISSN 1824-8039 . Published by SISSA Medialab.

https://pos.sissa.it/

PoS(EPS-HEP2025)232

1. Experimental status of all-charm tetraquark candidates

With the Run 2 dataset, ATLAS, CMS and LHCb have made progress in searching for all-charm tetraquark candidates [1–3]. All three experiments observed $X(6900)$ [also denoted $T_{cc\bar{c}\bar{c}}(6900)^0$ [4]], while CMS further claimed two additional structures: $X(6600)$ [$T_{cc\bar{c}\bar{c}}(6600)^0$] with 7.9σ significance and $X(7100)$ [$T_{cc\bar{c}\bar{c}}(7100)^0$] with 4.7σ significance. Interference effects were considered in the three experiments with different models, but the significances are all below 5σ. A near-threshold enhancement was also seen, but its nature remained unclear.

Many open questions remain, the most critical being whether these states and their interferences can be firmly established with higher statistical precision. Another key question is whether they can be observed in alternative decay channels. The larger dataset collected by CMS in 2022–2024 provides a more sensitive probe to confirm their existence, quantify interference effects, refine the measurements of their parameters, and potentially gain insights into the nature of these structures.

2. Updated CMS $J/\psi J/\psi$ analysis with combined Run 2 and Run 3 dataset

The combined Run 2 and Run 3 dataset corresponds to a total integrated luminosity of 315 fb^{-1}, including 135 fb^{-1} from Run 2 (2016–2018) and 180 fb^{-1} from Run 3 (2022–2024). The analysis focuses on the decay channel $J/\psi J/\psi \to \mu^+\mu^-\mu^+\mu^-$. The offline event selection for Run 3 follows the same criteria as for Run 2 [2], with the only major difference being the trigger. A new Run 3 trigger [5] requiring only two muons per event, instead of three as in Run 2, is the main driver of the increased signal yield. Consequently, the $J/\psi J/\psi$ rate rises from 93 events/fb^{-1} in Run 2 to 177 events/fb^{-1} in Run 3.

To fit the $J/\psi J/\psi$ invariant-mass distribution, both signal and background models are constructed, following those of the Run 2 analysis [2]. The signal process $X \to J/\psi J/\psi \to \mu^+\mu^-\mu^+\mu^-$ is simulated with JHUGen [6] and PYTHIA [7]. Each resonance is described by a relativistic S-wave Breit-Wigner (BW) function [8]: BW_1, BW_2, and BW_3 for $X(6600)$, $X(6900)$, and $X(7100)$, respectively. The background model includes several components: nonresonance single-parton scattering (NRSPS), double-parton scattering (DPS), combinatorial background (Comb), feed-down, and a near-threshold enhancement (BW_0). MC simulations with PYTHIA are performed to model the NRSPS and feed-down backgrounds. The parameterization of DPS is derived from the event-mixing of data. As for the combinatorial background, it is estimated by the data-driven "Nine tile" method [5]. The near-threshold enhancement is treated as background due to its unclear nature, and modeled by a BW function convolved with resolution function R. The complete background model is:

$$\begin{aligned} \text{Model}_{\text{bkg}}(m) &= N_{\text{BW}_0} \cdot f_{\text{BW}_0}(m) \otimes R_0(m) + N_{\text{NRSPS}} \cdot f_{\text{NRSPS}}(m) \\ &+ N_{\text{DPS}} \cdot f_{\text{DPS}}(m) + N_{\text{Comb.}} \cdot f_{\text{Comb.}}(m) + N_{\text{feed-down}} \cdot f_{\text{feed-down}}(m), \end{aligned} \tag{1}$$

where N_i refers to the yield and f denotes the probability density function of contributions i (the specific parameterizations are discussed in Ref. [5]).

Both no-interference and interference scenarios are considered in fitting the double J/ψ invariant-mass spectrum. In the no-interference model, the signal is described as the sum of three resonances: $\sum_{i=1}^{3} N_i \cdot |\text{BW}_i|^2 \otimes R_i$. In the interference model, the three peaks are allowed to

PoS(EPS-HEP2025)232

interfere, with the signal parameterized as $N_{\text{sig}} \cdot |r_1 \cdot e^{i\phi_1} \cdot \text{BW}_1 + \text{BW}_2 + r_3 \cdot e^{i\phi_3} \cdot \text{BW}_3|^2$, where r_i and ϕ_i are the relative magnitude and phase angle of BW_i with respect to BW_2. In both cases, the background model follows Eq. 1.

Likelihood fits are performed on data with both no-interference and interference models in the $J/\psi J/\psi$ invariant-mass range of 6-15 GeV. The results are shown in Fig. 1 (left and middle) and Tab. 1. The no-interference model fails to capture the features observed in the data, particularly the two dips between the three structures. The significance of these dips are evaluated from the likelihood difference between the full fit and a fit with the corresponding interference term removed. The significance of the dip between $X(6600)$ and $X(6900)$ is determined to be 9.7σ, and that between $X(6900)$ and $X(7100)$ is 6.5σ. Notably, even with the Run 3 dataset alone, the significances of the three resonances and two dips exceed 5σ.

With the increased data, the statistical uncertainties on the parameters of the three structures are reduced by about a factor of three in most cases, and the systematic uncertainties are also substantially reduced. In the interference fit, the local significances of $X(6600)$, $X(6900)$, and $X(7100)$, obtained from the likelihood difference with and without the respective contributions, are 15.2σ, 16.7σ, and 7.7σ. This study establishes, for the first time, all three structures $X(6600)$, $X(6900)$, and $X(7100)$, together with their interference, at significances well above 5σ.

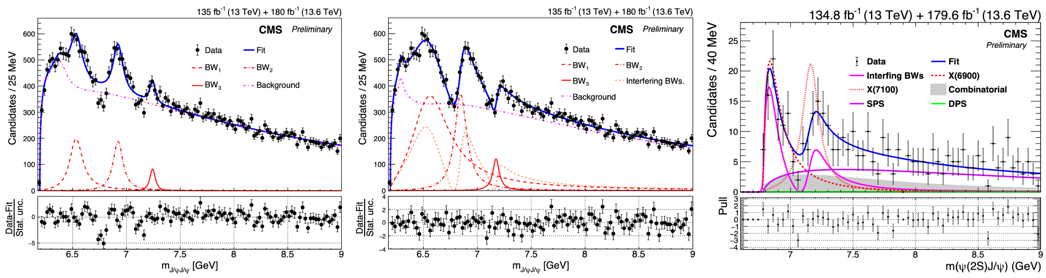

Figure 1: The $J/\psi\ J/\psi$ invariant-mass distribution along with the no-interference model (left), and the interference version (middle) [5]. Right: The $J/\psi\ \psi(2S)$ invariant-mass distribution along with the interference model (right) [9]. The fits are performed up to 15 GeV range, with zoomed views only up to 9 GeV being shown.

Table 1: Fit results for the masses M and widths Γ of three signal peaks shown for the $J/\psi J/\psi$ no-interference and interference models [5], as well as for the $J/\psi\psi(2S)$ interference model [9]. The no-interference results are statistical uncertainties only, while the interference results quotes statistical and systematic uncertainties in sequence.

	$J/\psi J/\psi \to \mu^+\mu^-\mu^+\mu^-$				$J/\psi\psi(2S) \to \mu^+\mu^-\mu^+\mu^-$	
	No-interference		Interference		Interference	
	M [MeV]	Γ [MeV]	M [MeV]	Γ [MeV]	M [MeV]	Γ [MeV]
$X(6600)$	6540 ± 8	142 ± 19	$6593^{+15}_{-14} \pm 25$	$446^{+66}_{-54} \pm 87$	–	–
$X(6900)$	6927 ± 6	97 ± 13	$6847^{+10}_{-10} \pm 15$	$135^{+16}_{-14} \pm 14$	$6876^{+46+100}_{-29-100}$	$253^{+290+120}_{-100-120}$
$X(7100)$	7247 ± 8	37 ± 24	$7173^{+9}_{-10} \pm 13$	$73^{+18}_{-15} \pm 10$	7169^{+26+74}_{-52-70}	$154^{+100+140}_{-82-160}$

PoS(EPS-HEP2025)232

3. Exploration of the $J/\psi\psi(2S)$ channel

Since $\psi(2S)$ is the radial excitation of J/ψ, if the observed structures correspond to genuine resonances, they are likely to decay into $J/\psi\psi(2S)$. A study of the $J/\psi\psi(2S) \to \mu^+\mu^-\mu^+\mu^-$ decay channel is conducted using the Run 2 and Run 3 data [9]. With the combined dataset, the statistics of $J/\psi\psi(2S)$ events obtained from a two-dimensional fit increase by a factor of about 2.5 compared to Run 2 alone.

The background contributions from NRSPS, DPS, and combinatorial sources are included. A signal model with the interference of two BW structures is considered since the mass of $X(6600)$ is below the mass threshold of $J/\psi\psi(2S)$. A likelihood fit is performed to the $J/\psi\psi(2S)$ invariant-mass spectrum. The results are shown in Fig. 1 (right) and Tab. 1. A prominent structure near the threshold is established with a local significance well above 5σ, and a structure in the higher-mass region is reported with a local significance of 4σ. These states are consistent with $X(6900)$ and $X(7100)$ observed in the $J/\psi J/\psi$ decay channel.

4. Spin-parity measurement of $J/\psi J/\psi$ structures

The observation of these tetraquark candidates has triggered intense theoretical interest. Various interpretations have been proposed, including hadronic molecules, compact tetraquarks, hybrids, and kinematic threshold effects. However, the true nature of these states remains unknown. Determining their spin and parity is crucial for discriminating among competing theoretical models.

The spin-parity measurement of the three tetraquark candidates, $X(6600)$, $X(6900)$, and $X(7100)$, is performed in the $J/\psi J/\psi \to \mu^+\mu^-\mu^+\mu^-$ decay channel using CMS Run 2 dataset, with the same event selection as in the $J/\psi J/\psi$ mass analysis [2]. The spin-parity determination relies on angular observables, which can be categorized into production and decay angles, as defined in Ref. [6]. The analysis uses decay angles only, while production angles are excluded to reduce model dependence. The production angular distributions are evaluated and found to be compatible with the unpolarized case.

Motivated by the strong interference observed in data, the spin-parity measurement is performed under the assumption that the three structures share the same spin and parity. Different spin–parity hypotheses are tested, including spin 0, 1, and 2 with both parities. As illustrated in Ref. [10], for a spin-0^+ particle decaying into two vector bosons via a parity-conserving interaction, two tensor structures are possible, denoted 0^+_m (minimal scalar coupling) and 0^+_h (higher-dimensional scalar coupling); their mixture (0^+_{mix}) is also examined. Similarly, two models, 2^-_m and 2^-_h, together with their mixture (2^-_{mix}), are considered for the spin-2^- hypothesis. For 0^-, 1^-, and 1^+, there is only one model for each case. For spin 2^+, four degrees of freedom are possible, and one representative model, 2^+_m, is tested, which includes all allowed polarizations, particularly those unique to the spin-2^+ scenario.

Instead of performing a multidimensional fit with all decay angles, an optimal discriminant $\mathcal{D}_{ij}$ is constructed to separate two spin-parity scenarios i and j, defined through the likelihood ratio of these two hypotheses [6]. The distribution of the discriminant to separate the 2^+_m and 0^- hypotheses is shown in Fig. 2 (left). A two-dimensional model, $\mathcal{P}_{ij}(m_{4\mu}, \mathcal{D}_{ij})$, incorporating the $J/\psi J/\psi$ invariant mass and discriminant, is employed to fit the data. The test statistic is calculated

PoS(EPS-HEP2025)232

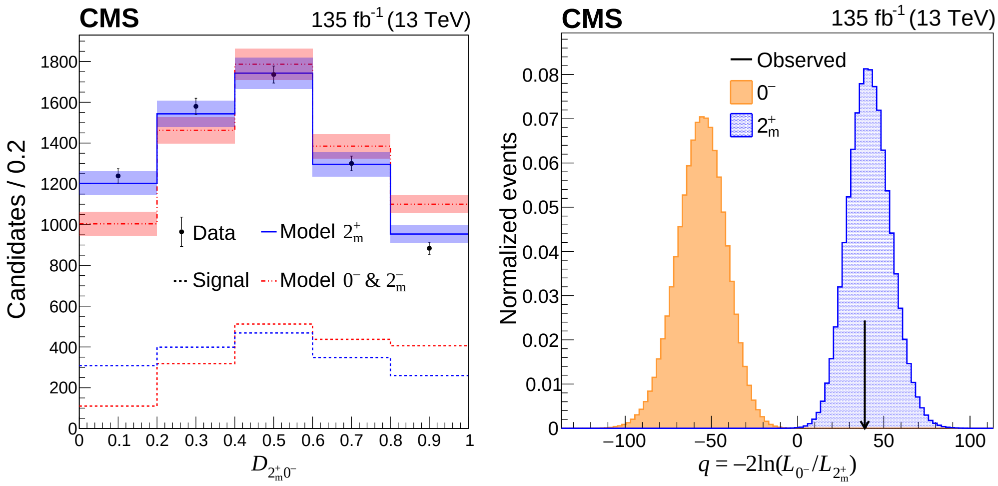

Figure 2: The distribution of discriminant $\mathcal{D}_{2^+_m 0^-}$ to separate spin-parity hypotheses 2^+_m and 0^- in the $J/\psi J/\psi$ invariant-mass range below 8 GeV (left). The distributions of test statistic $q = -2\ln(\mathcal{L}_{0^-}/\mathcal{L}_{2^+_m})$ for toy MC samples generated based on 2^+_m and 0^- hypotheses (right). The observed value is represented by the black arrow [10].

as $q = -2\ln(\mathcal{L}_{J_i^P}/\mathcal{L}_{J_j^P})$ when testing J_i^P hypothesis against J_j^P, where $\mathcal{L}$ denotes the likelihood value from the two-dimensional likelihood fit with $\mathcal{P}_{ij}(m_{4\mu}, \mathcal{D}_{ij})$. The hypotheses test between 2^+_m and 0^- is illustrated in Fig. 2 (right), where the 0^- hypothesis is clearly disfavored by the data. Similar hypothesis tests are performed for all spin–parity combinations. In all tests against 2^+_m, the alternative hypothesis is rejected. In brief, negative-parity scenarios are excluded at more than 3σ, spin-1^+ hypothesis at the 99% confidence level, and spin-0^+ hypothesis at the 95% confidence level. Higher-spin assignments are possible, but they are less likely due to the higher-energy requirement, making the spin-2^+ interpretation preferred by the data.

5. Conclusion and discussion

A set of comprehensive studies on all-charm tetraquarks has been carried out at CMS. Three tetraquark candidates, $X(6600)$, $X(6900)$, and $X(7100)$, are firmly established with significances well above 5σ with the combined Run 2 and Run 3 datasets. Furthermore, two of these states, $X(6900)$ and $X(7100)$, are independently confirmed in the $J/\psi\psi(2S) \to \mu^+\mu^-\mu^+\mu^-$ channel. Additionally, interference effects between these states are observed in the $J/\psi J/\psi$ channel with significances exceeding 5σ, implying that these states share the same quantum numbers. Under this premise, a spin-parity measurement has been conducted using the CMS Run 2 dataset which indicates a preference for a 2^{++} spin-parity assignment. Notably, large mass splittings (> 200 MeV) between these states are observed, which exceed typical spin–orbital splittings and are comparable to some of those in the Υ family ($1S$, $2S$, $3S$ radial excitations). Moreover, their absolute masses appear to form a Regge trajectory [11]. These features collectively point to a coherent picture in which these states form a family of all-charm tetraquarks [12, 13] with a diquark-antidiquark structure, where both diquarks are in a spin-1 state [14]. Further explorations, such as searches in

PoS(EPS-HEP2025)232

additional decay channels and the cross-section measurements, will provide more insights to clarify the intrinsic nature of these intriguing states.

References

[1] ATLAS Collaboration. *Observation of an excess of dicharmonium events in the four-muon final state with the ATLAS detector*. *Phys. Rev. Lett.*, **131**:151902, 2023.

[2] CMS Collaboration. *New structures in the $J/\psi J/\psi$ mass spectrum in proton-proton collisions at $\sqrt{s}$=13 TeV*. *Phys. Rev. Lett.*, **132**:111901, 2024.

[3] LHCb Collaboration. *Observation of structure in the J/ψ-pair mass spectrum*. *Sci. Bull.*, **65**:1983, 2020.

[4] Particle Data Group. *Review of particle physics*. *Phys. Rev. D*, **110**:030001, 2024.

[5] CMS Collaboration. *Observation of a family of all-charm tetraquark candidates at the LHC*. https://cds.cern.ch/record/2929472/files/BPH-24-003-pas.pdf.

[6] Y. Gao, A. V. Gritsan, Z. Guo, K. Melnikov, M. Schulze, and N. V. Tran. *Spin determination of single-produced resonances at hadron colliders*. *Phys. Rev. D*, **81**:075022, 2010.

[7] T. Sjostrand, S. Mrenna, and P. Z. Skands. *A brief introduction to PYTHIA 8.1*. *Comput. Phys. Commun.*, **178**:852, 2008.

[8] A. R. Bohm and Y. Sato. *Relativistic resonances: their masses, widths, lifetimes, superposition, and causal evolution*. *Phys. Rev. D*, **71**:085018, 2005.

[9] CMS Collaboration. *Observation of X(6900) and evidence of X(7100) in the $\psi(2S)J/\psi$ to 4μ mass spectrum in pp collisions at CMS*. https://cds.cern.ch/record/2929529/files/BPH-22-004-pas.pdf.

[10] CMS Collaboration. *Determination of the spin and parity of all-charm tetraquarks*. arXiv:2506.07944 [hep-ex], CMS-BPH-24-002, CERN-EP-2025-118 (2025). Submitted to *Nature*.

[11] F. Zhu, G. Bauer, and K. Yi. *Experimental road to a charming family of tetraquarks . . . and beyond*. *Chin. Phys. Lett.*, **41**:111201, 2024.

[12] R. Zhu. *Fully-heavy tetraquark spectra and production at hadron colliders*. *Nucl. Phys. B*, **966**:115393, 2021.

[13] R. Tiwari, D. P. Rathaud, and A. K. Rai. *Spectroscopy of all charm tetraquark states*. *Indian J. Phys.*, **97**:943, 2023.

[14] I. Belov, A. Giachino, and E. Santopinto. *Fully charmed tetraquark production at the LHC experiments*. *JHEP*, **01**:093, 2025.

PoS(EPS-HEP2025)232